CESARE'17
COORDINATING ENGINEERING FOR SUSTAINABILITY AND RESILIENCE
Dead Sea, Amman, Jordan
3-8 May 2017
JORDAN UNIVERSITY OF SCIENCE & TECHNOLOGY
IRBID - JORDAN

REVIEW OF AASHTO WATER FLOW DRAG COEFFICIENTS USING FINITE ELEMENT METHOD

Amin H. Almasri [1, 2], and Shadi Moqbel [3]

[1]Department of Civil Engineering
Jordan University of Science and Technology
Irbid, 22110, Jordan (on sabbatical leave)
e-mail: ahalmasri@just.edu.jo

[2]Department of Civil Engineering
Fahad Bin Sultan University
Tabuk, Saudi Arabia
e-mail: aalmasri@fbsu.edu.sa

[3]Department of Civil Engineering
The University of Jordan
Amman, Jordan
e-mail: s.moqbel@ju.edu.jo

Keywords: Drag coefficients, water flow, finite element method.

Abstract. *Water flow usually applies a dynamic force to obstacles that exist in their way. This force is calculated empirically based on drag coefficients stated in design codes and specifications. Different values of drag coefficients have been reported in literature. For example, AASHTO LRFD Bridge Design Specifications uses a drag coefficient of 1.4 and 0.7 for square-ended and semicircular-nosed pier, respectively, while Coastal Construction Manual (FEMA P-55) recommends a value of 2 and 1.2 for square and round piles, respectively. In addition, many researchers have obtained other different values of drag coefficient under similar conditions (i.e. similar range of Reynolds number) reaching to 2.6 for square object. The present study investigates the drag coefficient of flow around square, 90o wedged-nosed and circular piers numerically using finite element method. Results showed that AASHTO values for drag force coefficient varied between very conservative to be under-reckoning. The study recommends that AASHTO drag coefficient values should be revised for different circumstances and under more severe conditions.*

1 INTRODUCTION

The intensive use of vehicles in daily life and the race to reach destination in a short time and in the most economical way had resulted in laying roads in an unprecedented rate especially in the developing countries. Following this race to laying roads, bridges are being built over valleys and water paths. Bridge piers in these water paths can reach depths of 10's of meters. Designing these piers includes different parameters for various forces and stresses calculations.

These piers are susceptible to drag force resulting from water movement. Design codes have specific provisions on how to calculate the effect of this force on specific bridge pier shape depending on a constant drag coefficient (CD). However, this drag coefficient of any object is known to be function of fluid density and viscosity, flow speed and direction, and object position, shape, and size. Fluid velocity, fluid kinematic viscosity and object size are incorporated into a dimensionless quantity called the Reynolds number. Therefore, drag coefficient is highly dependent on Reynolds number. Different values of drag coefficient can be found in literature for the same problem leaving designers in a dilemma on which drag factor is appropriate. For example, AASHTO LRFD Bridge Design Specifications [1] states a drag coefficient of 1.4 and 0.7 for square-ended and semicircular-nosed pier, respectively, while Coastal Construction Manual (FEMA P-55) [2] recommends a value of 2 and 1.2 for square and round piles, respectively.

In this study the drag force coefficient for various pier shapes is estimated numerically using computational fluid dynamics within the finite element software ABAQUS/CFD. The values obtained cover conditions from still water to fast river flow with different inclination angle. Then, the drag coefficient values were compared to AASHTO design code and available literature values.

2 METHODOLOGY

This study concentrates on water flowing under natural conditions simulating river streams and lakes. Therefore, bridge pier shapes were simulated over wide range of flow velocity covering conditions of nearly still water to flow velocity experienced in flash floods. To achieve this goal, the finite element software ABAQUS/CFD was used with its computational fluid dynamics solving capabilities.

The drag force is calculated in the software by integrating the pressure profile over the area. It can be calculated in the flow direction as well as the direction perpendicular to the flow. Generally, the drag coefficients can be calculated through the following relationships:

$$C_d = \frac{F_x}{\frac{1}{2}V^2 A_d} \tag{1}$$

where C_d is drag coefficient in longitudinal direction, F_x is drag force parallel to the flow direction, V is flow design velocity, A_d is the area of the edge perpendicular to longitudinal axis of pier. Reynolds number (R_e) is obtained through the relation:

$$R_e = \frac{\rho v L}{\mu} \tag{2}$$

where L is a characteristic length of the object, which will be the pier width in this case. ρ is the water density, v is the flow velocity, and μ is the dynamic viscosity of water.

3 RESULTS AND DISCUSSION

Drag coefficient is obtained for square pier at velocities of 0.001, 0.01, 0.1, 1, 3, and 5 m/s, representing flow velocities of almost still water to fast river flow. Figure 1 show the pressure contours at the typical velocities of 1 m/s, where flow is perpendicular to pier surface. Pressure contour at velocity 1 m/s shows the formation of vortices behind the pier, which is why pressure contour is not symmetric. They usually form in turbulent flow behind the piers. Vortex initiation results from the interaction of two streams that were separated from the original stream due to the obstacle (pier), after solving Navier-Stokes equations.

The change in drag coefficient with Reynolds number is plotted in Fig.2. The current results are seen to be considerably less than most of the results obtained by other researchers (Wenxiu et al. [2013], He et al. [2014], Yamagishi et al. [2009], Dutta et al. [2008], and Sohankar et al. [1999]) under similar circumstances (i.e. similar Reynolds number range, for water flow). Results in literature obtained for gas flow or at lower Reynolds number are believed not to be suitable for comparisons purposes here, and hence are not included. Current study results of drag coefficient are noticed to coincide with AASHTO results of 1.4 at Reynolds numbers ranging from 10^4 to 10^6, and deviate out of this range of Reynolds numbers. The drag coefficient is found to be about 1.8 at Reynolds number of 1000, which is at a flow velocity of 0.001m/s. This can be neglected for pier design purposes since it represents still water, and will not cause any significant force on the pier. However, when Reynolds number is higher than 10^6, the drag coefficient is seen to be higher than the AASHTO value, and could reach to 1.6 for a flow velocity of 5 m/s, which can occur in some rivers or flash floods. Therefore, the AASHTO value might not be safe for this higher range of flow velocities.

Drag coefficient of wedged-nosed pier is also studied here, and illustrated in Fig. 3 for different tail lengths at a flow velocity of 1 m/s. The figure shows that the drag coefficient reduces with increasing pier tail length, approaching a value of 0.7 for a considerably long pier compared to its width. The AASHTO value is 0.8 in this case. However, the drag coefficient rises to about 1.3 for a fully wedged pier at this water velocity.

The change in drag coefficient with Reynolds number is plotted in Fig. 4 for circular pier. The current results are seen to be equal to or less than most of the results documented by other researchers (Hughes and Brighton [1999], Wang et al. [2001], Hinsberg et al. [2014], Tsutsui [2008], and Sato and Kobayashi [2012]) for Reynolds number ranging from 103 to 107, which covers the typical values of water flow pressuring circular bridge piers. It reaches a value of 0.45 at high Reynolds number, which is less than the semicircular nosed pier value of about 0.7. Hence, using the AASHTO semicircular nosed pier drag coefficient for fully circular piers will be very conservative. However, the current results of drag coefficient rises quickly for Reynolds number below 103 and diverge from other researchers values, but this range of Reynolds number is beyond the interest of this research. It is worth noting that experimental results on flow around circular cylindrical shapes usually show a dramatic drop in the drag coefficient between Reynolds number of 10^5 and 10^6 as a result of the change in the location of the separation point and reduction in the wake and negative pressure behind the pier. This phenomenon was translated into switching the flow regime from subcritical flow to supercritical flow, and was not captured in this study.

4 CONCLUSIONS

The present paper studies numerically the drag force and coefficient values of water flow for different pier shapes, and compares the results with AASHTO Bridge Design Code values as well as with values obtained by other researchers. The following conclusions can be drawn:

1. The AASHTO longitudinal drag coefficient value of 1.4 for square piers might not be safe for high Reynolds numbers, which represent high river flow velocities.

2. The drag coefficient for wedged-nosed pier suggested in AASHTO agrees well with the numerically obtained one, only for a pier long enough compared to its width. For wedged-nosed piers with tail length to width ratio less than 3, a value higher than that in the AASHTO should be used.

3. The effect of one pier on another should be studied and included in the design codes as it could lead to higher forces on the piers that are not accounted for by the current design methodologies. It could lead to piers failure due to the underestimation of these forces.

5 REFERENCES

[1] AASHTO, (2013) "AASHTO LRFD Bridge Design Specifications, 6th edition.

[2] FEMA P-55, (2011). Coastal Construction Manual: Principles and Practices of Planning, Siting, Designing, Constructing, and Maintaining Residential Buildings in Coastal Areas, 4th Edition

[3] Wenxiu, L., Bing, Z. and Xulin, H. (2013). "Two-dimensional Numerical Simulation of Drag Coefficients on Two Square Cylinders at High Reynolds Number". 2nd International Conference on Intelligent System and Applied Material (GSAM 2013), EDUGAIT Press.

[4] Tsutsui, T. (2008). "Fluid Force Acting On A Cylindrical Pier Standing In A Scour". BBAA VI International Colloquium on: Bluff Bodies Aerodynamics & Applications Milano, Italy, July, 20-24.

[5] Sato, M. and Kobayashi, T. (2012). "A fundamental study of the flow past a circular cylinder using Abaqus/CFD". SIMULIA Community Conference, May 15-17, 2012 - Providence RI, USA

[6] Sohankar, A., Norberg, C. and Davidson L. (1999) "Simulation of three-dimensional flow around a square cylinder at moderate Reynolds numbers". Physics of Fluids, Vol. 11, No. 2.

[7] Dutta, S., Panigrahi, P., and Muralidhar, K., (2008) "Experimental Investigation of Flow Past a Square Cylinder at an Angle of Incidence". Journal of Engineering Mechanics, Volume 134, Issue 9, pages (788-803).

[8] He, G., Li, N., and Wang, J. (2014). "Drag reduction of square cylinders with cut-corners at the front edges". Experiments in Fluids, Vol. 55, page 1745.

[9] Yamagishi, Y., Kimura, S., Oki, M., and Hatayama, C., (2009). "Effect of Corner Cutoffs On Flow Characteristics Around A Square Cylinder," 10th International Conference on Fluid Control, Measurements, and Visualization. Mosco, Russia

[10] Hughes, W.F., & Brighton, J.A., (1999). "Schaum's outline of fluid dynamics," USA: McGraw-Hill, pp.102.

[11] Wang, M., Catalano, P., AND Iaccarino, G., (2001). "Prediction of high Reynolds number flow over a circular cylinder using LES with wall modeling," Center for Turbulence Research, Annual Research Briefs. pp. 45-50.

[12] Hinsberg, N., Lueckhof, J.M., Nuhn, J., (2014). "The Reynolds number effect from subcritical to high transcritical on steady and unsteady loading on a rough circular cylinder," Proceedings of the 9th International Conference on Structural Dynamics, EURODYN 2014, Porto, Portugal, 30 June - 2 July 2014, pp. 3211- 3218.

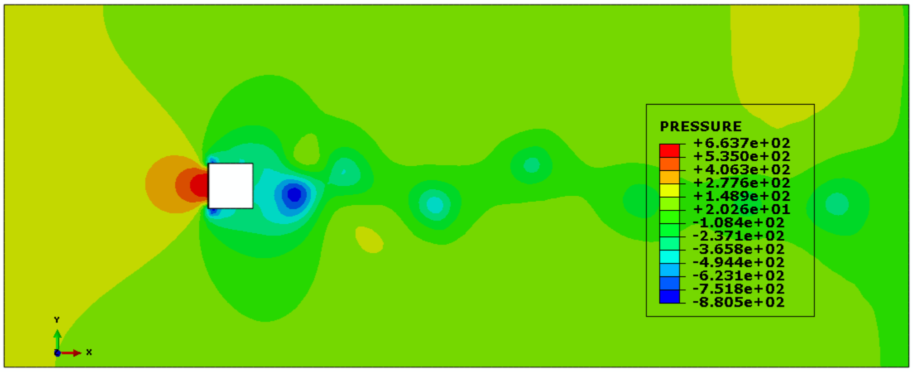

FIG. 1: Pressure contours at velocity of 1m/s for square pier

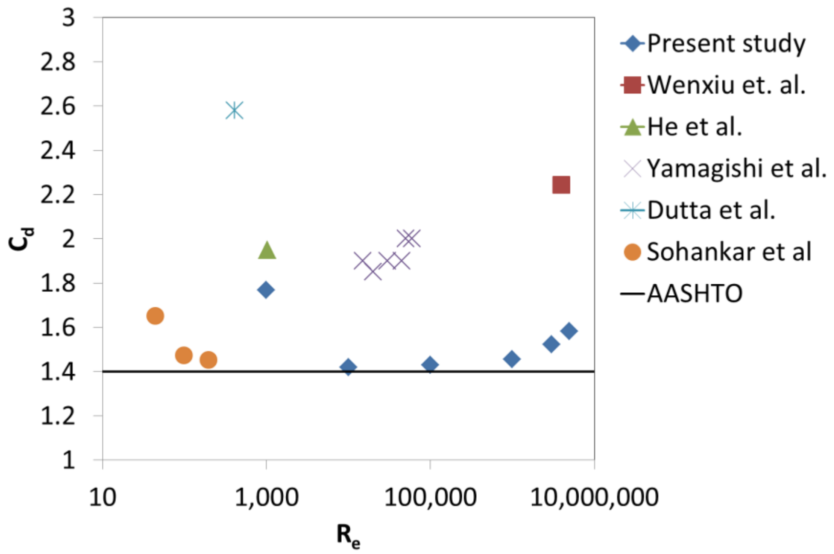

FIG. 2: Longitudinal drag coefficient at different Reynolds numbers for square pier.

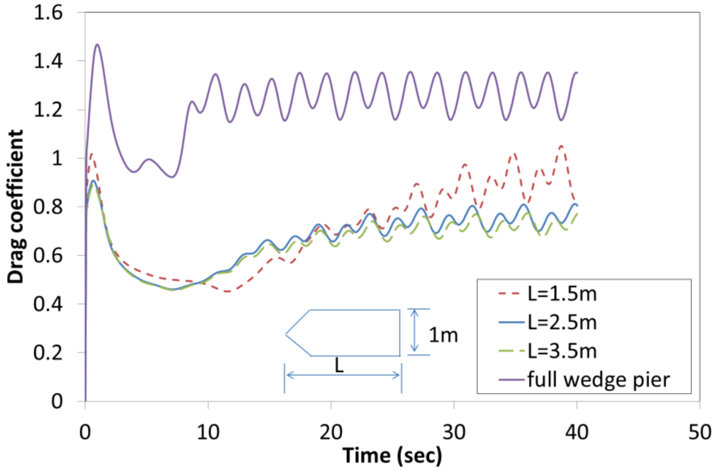

FIG. 3: Longitudinal drag coefficient for wedged-nosed pier.

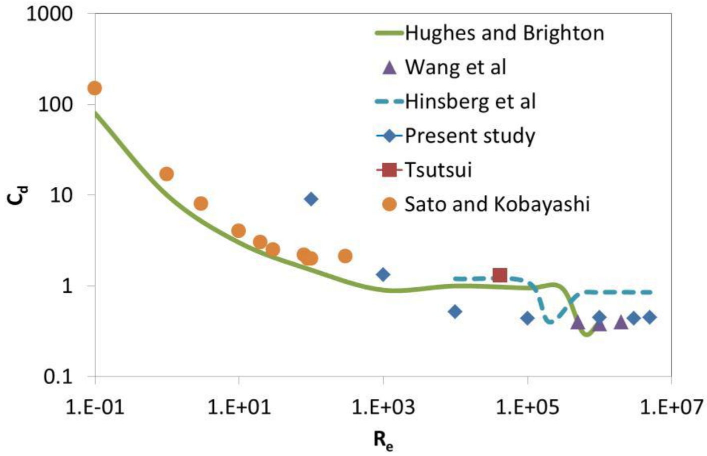

FIG. 4: Drag coefficient versus Reynolds number for circular pier.